E. coli Inactivation by High-Power Impulse Magnetron sputtered (HIPIMS) Cu surfaces

ARTICLE *in* THE JOURNAL OF PHYSICAL CHEMISTRY C · NOVEMBER 2011

Impact Factor: 4.77 · DOI: 10.1021/jp204503y

9 AUTHORS, INCLUDING:

Ewelina Kusiak-Nejman
West Pomeranian University of Technology, …
21 PUBLICATIONS **242** CITATIONS
SEE PROFILE

Antoni W Morawski
272 PUBLICATIONS **4,626** CITATIONS
SEE PROFILE

César Pulgarin
École Polytechnique Fédérale de Lausanne
371 PUBLICATIONS **7,982** CITATIONS
SEE PROFILE

J. Kiwi
École Polytechnique Fédérale de Lausanne
328 PUBLICATIONS **10,915** CITATIONS
SEE PROFILE

THE JOURNAL OF PHYSICAL CHEMISTRY C

ARTICLE

pubs.acs.org/JPCC

E. coli Inactivation by High-Power Impulse Magnetron Sputtered (HIPIMS) Cu Surfaces

E. Kusiak-Nejman,[†,‡] A.W. Morawski,[‡] A. P. Ehiasarian,[§] C. Pulgarin,[†] O. Baghriche,[†] E. Mielczarski,[∥] J. Mielczarski,[∥] A. Kulik,[⊥] and J. Kiwi*[,#]

[†]Group of Electrochemical Engineering, EPFL-SB-ISIC-GGEC, Station 6, CH-1015, Lausanne, Switzerland

[‡]West Pomerianian University of Technology, Szczecin, Institute of Chemical and Environment Engineering, Pulaskiego 10, 70-322 Szczecin, Poland

[§]Material and Engineering Research Institute, Sheffield Hallam University, Howard St. Sheffield, S1 1WB, U.K.

[∥]INPL/ENG, CNRS, UMR7569, Pole de l'Eau, BP 40,15 Av du Charmois 54501Vandoeuvre-les-Nancy, Cedex, France

[⊥]EPFL SB IPSB LPMV BSP 417, Bât. sciences physiques UNIL, CH-1015, Lausanne Switzerland

[#]Laboratory of Photonics and Interfaces, EPFL-SB-ISIC-LPI, Chemistry Building, Station 6, CH-1015, Lausanne, Switzerland

ABSTRACT: This study reports HIPIMS-sputtered samples of Cu-particulate films with currents at 6 and 60 amps leading to *E. coli* inactivation. The Cu coverage and nanoparticle structure of the fibers is reported by TEM. Evidence is presented of redox processes in the Cu taking place during *E. coli* inactivation and the buildup of intermediate species resulting from the bacterial oxidation. Cu is deposited on the polyester in the form of Cu_2O and CuO as observed by XPS. During the bacterial oxidation, the CuO on the polyester after 30 min decreases from 84 to 70%. After longer bacterial inactivation times, the CuO oxidizes again increases its presence to 94% when the bacterial inactivation has been completed within 90 min. The broadening of the O−C═O signal during *E. coli* inactivation suggests direct interaction of Cu with carboxylic groups. The surface atomic concentration of O, Cu, and C was determined within the *E. coli* inactivation time. The *E. coli* inactivation occurred within 90 min on Cu-nanoparticulate films sputtered for 61 s at 60 amps being 28 nm thick. This Cu-layer thickness is equivalent to 140 layers with a content of 1.4×10^{17} atoms Cu/cm^2, and the sputtering proceeded with deposition rate of 2.3×10^{15} atoms/cm^{2}s. The values found for the rugosity indicate that the texture of the Cu-nanoparticulate film is smooth. R_q values and the R_a were similar before and after the *E. coli* inactivation, providing further evidence of the stability of the Cu-nanoparticulate films during the bacterial inactivation process. The Cu-loading percentage required in the Cu-nanoparticulate films sputtered by HIPIMS to inactivate *E. coli* completely was about three times lower compared with DCMS-sputtered Cu-nanoparticulate films. This indicates a substantial Cu-metal savings within the preparation of antibacterial films.

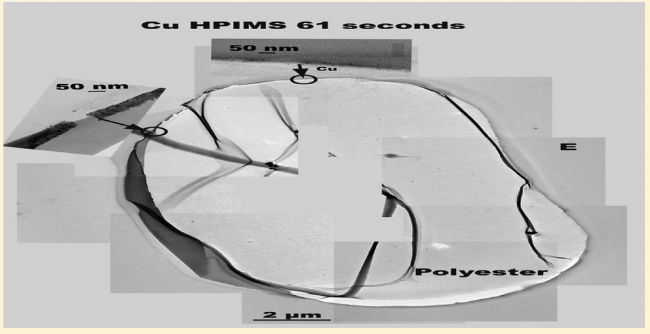

INTRODUCTION

The field of antibacterial Cu-films has gained much attention during the past decade.[1,2] Antimicrobial surfaces are interesting because they can reduce or eliminate hospital-acquired infections (HAIs) due to antibiotic-resistant bacteria that survive on hospital surfaces for long times.[3,4] Cu-bactericide properties have been known for decades[5] because of the release of metal ions into the surrounding fabrics. Cu films would avoid the use of chemicals to clean/disinfect rooms, leaving residues after use.[6]

Recently wet impregnation of Cu films on cotton has been reported.[7] Sputtering of highly active nanoparticles of Ag, Cu, Pt, Au, and Rh films have shown that the Cu film was the most effective antibacterial and antifungal film. No fouling was found on the Cu films and in the inhibition zone around the fabric for all microorganisms tried.[8] On the basis of this observation, the area of sputtering on medical devices is a current area of research.

The particular interest in Cu textiles is based on the fact that the porous hydrophilic structure of textiles provides a suitable environment for bacterial growth. Cu sputtering has shown to improve the antibacterial properties of textile substrates.[9] In recent years, PVD or more modern sputtering chambers have modified the structure of fibers, producing a variety of antimicrobial surfaces.[10−12] Reactive DC-sputtering of polyimide has been reported recently to bind Cu chemically to the substrate through a stable complex linkage.[13] Cu-based nanostructures with antibacterial properties have been reported recently by coordination precursors between Cu^{2+} and glycine.[14]

Received: May 14, 2011
Revised: August 4, 2011
Published: September 19, 2011

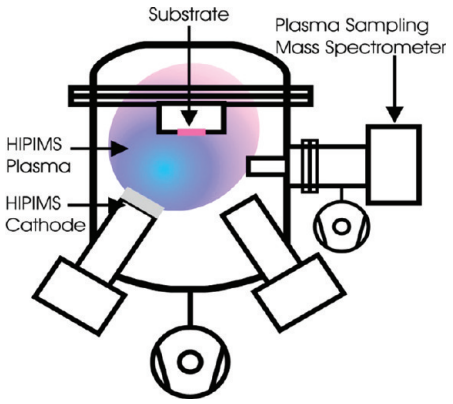

Figure 1. Schematic of the HIPIMS installation used; the cathode was Cu and the substrate was polyester.

Applications of antimicrobial Cu-nanoparticulate films have been reported recently by Gabbay and Borkow[15−17] and Gedanken.[18] These authors have prepared and evaluated Cu-impregnated surfaces with potential biocide activity. For some years, a technology has been developed to introduce Cu into natural and artificial fibers, latex, and polymer films. The applications of these fibers address the treatment of viral transmissions, nosocomial infections, and antibiotic-resistant bacteria.

Plasma-based film deposition processes have lately evolved toward the higher ionization of ion/metal in the plasma flux. This enhances the film uniformity, the production of highly ionized metal-ions, the film adherence, and compactness.[19−21] HIPIMS technology fulfills these requirements, producing high-power homogeneous plasma glow at high currents up to 2000 V and 10 amps.

In the case of direct current magnetron sputtering (DCMS) and DCMSP, the ionization of metals has been reported to be 1−5%, and the equilibrium potential given by the balance of electrons and metal ions is slightly positive,[22,23] but in HIPIMS, the ionization in the sputtering chamber reaches 50−90% and the highly ionized metal particles stick more readily to the substrate using the same negative bias voltage as in the case of DCMS and DCMPS-sputtering leading to different metal microstructures.[24]

Engineering of Cu-nanoparticulate films is an important area helping to reduce/eliminate the rate of HAI-type infections. We focus in this study on the deposition of Cu films using high-power impulse magnetron sputtering (HIPIMS) and compare the results obtained with recent work reported sputtering Cu on fabrics by DCMS,[25,26] where a lower Cu-ions/Cu^o flux is available in the sputtering chamber. The Cu films will be evaluated for *E. coli* inactivation, surface redox processes (XPS), and the surface microstructure. The Cu-polyester fabrics will be analyzed for the percentage of Cu by weight/cm^2 by X-ray fluorescence. The ionization percentage of Ar^+, Ar^{2+}, Cu^+, and Cu^{2+} will be quantified by gas-phase mass spectrometry for HIPIMS and DCMS. The microstructure of the Cu layers will be described by electron microscopy. The Cu-redox interfacial reactions following changes in the Cu-oxidation states take place concomitantly to the build-up of oxidative carbon-functionalities and were monitored by XPS.

EXPERIMENTAL SECTION

HIPIMS Sputtering on Polyester, Materials, and Cu-Film Calibration. HIPIMS deposition of Cu was carried out in a CMS-18 vacuum system from Kurt Leske evacuated to 10^{-5} Pa by a turbomolecular pump.[19] Figure 1 shows the scheme of the HIPIMS chamber. The Cu target was 5 cm in diameter, 99.99% pure from K. Lesker. The mass spectrometry measurements were carried out in a Hiden Analytical PSM003 unit to determine the ion composition of the ions in the plasma Ar atmosphere.[20] The HIPIMS was operated at 100 Hz with pulses of 100 microseconds separated by 10 ms. The HIPIMS short pulses avoided a glow-to-arc transition during plasma particle deposition.[21]

The polyester used corresponds to the EMPA test cloth sample no. 407. It is a polyester Dacron, type 54 spun, plain weave ISO 105-F04 used for color-fastness determinations.

The calibration of the Cu-nanoparticulate film thickness by HIPIMS on the Si wafers is shown in Figure 2. The film thickness was determined with a profilometer (Alphastep500, TENCOR). The values of the thicknesses of the Cu films for diverse sputtering times using HIPIMS are shown in Table 1. The calibration traces in Figure 2 presented a ±10−15% range of variation or experimental error. For 21 s of deposition time with 6 amps, a thickness of 28 nm was found. A deposition time of 61 s at 60 amps led to a 28 nm Cu layer (Table1).

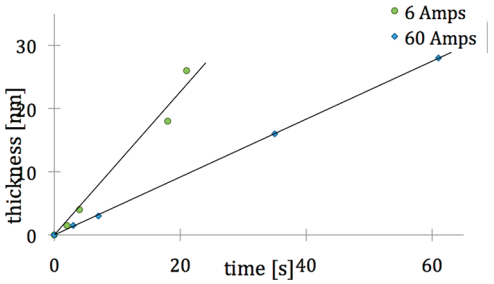

Figure 2. Nominal calibration of the Cu thickness layer when sputtering at 6 and 60 amps.

Table 1. Sputtering Time and Thickness of the Cu−Layers on Polyester by HIPIMS at 6 and 60 amps

	deposition time (s)	(amps)	thickness [nm]	Cu (wt %)
HIPIMS	2	6	1.5	0.0121
	4	6	4	0.0200
	18	6	16	0.0600
	21	6	28	0.1120
	3	60	1.5	0.0073
	7	60	3	0.0182
	35	60	16	0.0675
	61	60	28	0.1020

X-ray Fluorescence of Cu-Nanoparticulate Film (XRD). The Cu content of the most relevant samples of polyester/Cu during *E. coli* inactivation was evaluated by X-ray fluorescence. The spectrometer used was RFX, PANalytical PW2400. For the two most effective loadings of Cu on polyester, a deposition time of 21 s with 6 Amps led to 0.112 wt % Cu/wt polyester, and a deposition time of 61 s at 60 amps led to 0.102 wt % Cu/wt polyester.

Bacterial Inactivation of *E. coli* on Cu-Nanoparticulate Film. The samples of *Escherichia coli* (*E. coli* K12) were obtained from the Deutsche Sammlung von Mikroorganismen and Zellkulturen GmbH (DSMZ) ATCC23716 (Braunschweig, Germany) to test the antibacterial activity of the Cu-nanoparticulate films. The polyester fabrics were sterilized by autoclaving at 121 °C for 2 h. We placed a 20 μL aliquot of culture with an initial

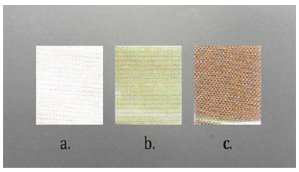

Figure 3. (a) Polyester alone and (b) Cu-HIPiMS-sputtered polyester for 7 s, 60 amps, and 3 nm thickness. (c) Cu-HIPiMS-sputtered polyester for 61 s, 60 amps, and 28 nm thickness.

concentration of 3.8×10^6 CFU mL^{-1} in NaCl/KCl on each coated and uncoated (control) polyester fabric. The samples were placed on a Petri dish provided with a lid to prevent evaporation. After each determination, the fabric was transferred to a sterile 2 mL Eppendorf tube containing 1 mL of autoclaved NaCl/KCl saline solution. This solution was subsequently mixed thoroughly using a vortex for 3 min. Serial dilutions were made in NaCl/KCl solution. A 100 μL sample of each dilution was pipetted onto a nutrient agar plate and then spread over the surface of the plate using standard plate method. Agar plates were incubated, lid down, at 37 °C for 24 h before colonies were counted. The bacterial data reported were replicated three times.

Electron Microscopy of Cu-Nanoparticulate Film (TEM). A Philips CM-12 (field emission gun, 300 kV, 0.17 nm resolution) microscope at 120 kV was used to measure the particles size of the Cu nanoparticles. The textiles were embedded in epoxy resin 45359 Fluka, and the fabrics were cross-sectioned with an ultramicrotome (Ultracut E) and at a knife angle at 35°. Images were taken in bright field (BF).

Atomic Force Microscopy of HIPIMS-Sputtered Samples (AFM). Measurements were performed with a Parks Scientific XE120 AFM in contact mode. The Cantilever used was an Olympus OMCL-TR400 with a spring constant of 0.02 N/m. Several images with a scanning field 5×5 μm were taken using a line frequency of 2 Hz. Images were flattened along the X axis, line-by-line by means of a second-order polynomial expression, and the roughness was calculated using Parks' XEI software.

X-ray Photoelectron Spectroscopy of Cu-Nanoparticulate Film (XPS). An AXIS NOVA photoelectron spectrometer (Kratos Analytical, Manchester, U.K.) equipped with monochromatic Al Kα ($h\nu$ = 1486.6 eV) anode was used. The electrostatic charge effects on the samples were compensated by means of the low-energy electron source working in combination with a magnetic immersion lens. The carbon C1s line with position at 284.6 eV was used as a reference to correct the charging effect. The quantitative surface atomic concentration of some elements was determined from peak areas using sensitivity factors.[27,28] The spectrum background was subtracted/corrected for electrostatic charging according to Shirley.[29] The XPS spectra for the Cu species were analyzed by means of spectra deconvolution software (CasaXPS-Vision 2, Kratos Analytical U.K.).

RESULTS AND DISCUSSION

Cu-Nanoparticulate Films Optical Absorption As a Function of Sputtering Time. Figure 3 shows the polyester alone in sample a shows no color in the absence of Cu. A light green color appears in sample b, indicative of Cu clusters deposited by HIPIMS for 7 s at 60 amps. Sample c shows brown metallic Cu color due to HIPIMS sputtering for 61 s at 60 amps. The darker color in sample c is due to the longer sputtering time allowing the Cu to diffuse anisotropically and aggregate, leading

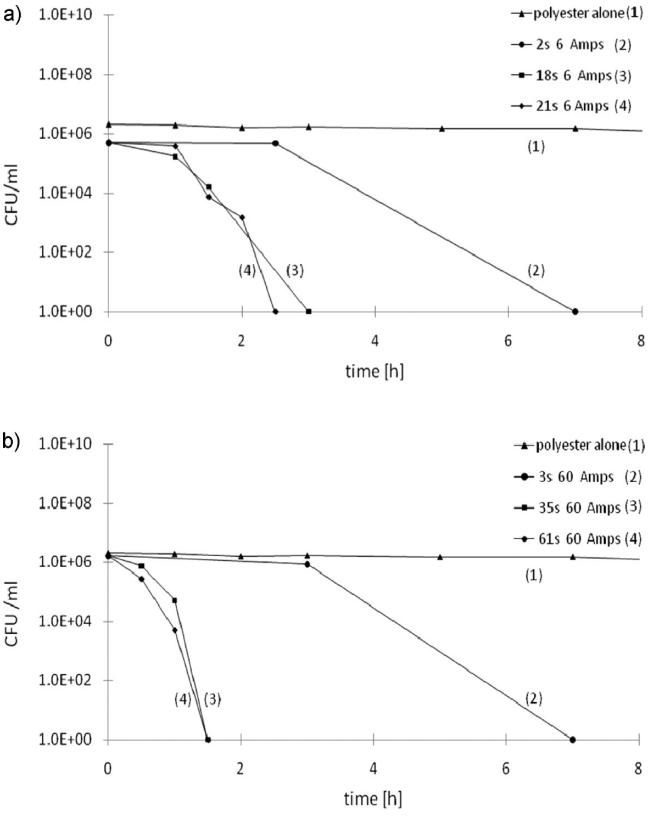

Figure 4. (a) Kinetics of the *E. coli* inactivation by HIPIMS Cu-deposited polyester with 6 amps. (b) Kinetics of the *E. coli* inactivation by HIPIMS Cu-deposited polyester with 60 amps.

to thermodynamically stable Cu agglomerates.[30,31] The color in Figure 3c corresponds to the species CuO with a band gap (b_g) of 1.7 eV and a flat band potential of −0.3 V versus SCE (pH 7) reaching an absorption edge of 725 nm.[32]

***E. coli* Inactivation Kinetics Mediated by HIPIMS-Deposited Cu on Polyester.** Figure 4a presents the results of HIPIMS sputtering of Cu on polyester with 6 amps between 2 and 21 s. The polyester sample did not lead to any *E. coli* inactivation, and the *E. coli* inactivation occurred within short times in Figure 4a with longer sputtering time. The initial CFU decrease in Figure 4a for Cu-nanoparticulate films at time zero with respect to polyester alone is due to redox processes between Cu and the *E. coli* occurring on the Cu-nanoparticulate film surface.[25,26]

Figure 4b presents the inactivation kinetics of *E. coli* mediated by Cu-nanoparticulate films between 3 and 61 s at 60 amps. It is readily seen that as the HIPIMS sputtering increases the times needed to inactivate *E. coli* become shorter. The times of sputtering and the energy applied were different from the ones used in Figure 4a. The higher energies of polyester sputtered with 60 amps may promote a faster migration of the sputtered Cu particles compared with HIPIMS at 6 amps. Also, a local softening of the fibers at the contact sites takes place at a higher sputtering energy and may play a significant role in the inactivation time of *E. coli* when sputtering with high currents as compared with lower currents because of the effect of higher temperatures available to the substrate.[33]

DCMS applied at 300 mA for 180 s[25] deposited Cu layers 16 nm thick with a Cu content of 0.294% that inactivated *E. coli* completely within 120 min in the dark. Applying HIPIMS with 6

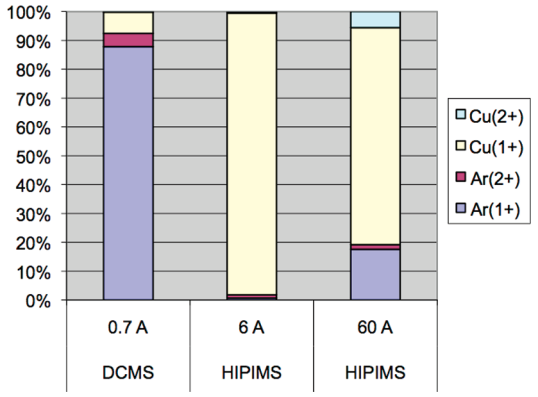

Figure 5. Ar-ion composition and Cu-ion composition determined mass spectrometry in the gas phase of a DCMS and an HIPIMS sputtering chamber. For other details, see the text.

amps for 21 s, Cu layers 28 nm thick were observed with a Cu content of 0.1120% that inactivated *E. coli* completely within 140 min in the dark (Table 1 and Figure 4a). Applying HIPIMS with 60 amps for 61 s, Cu layers 28 nm thick were observed with a Cu content of 0.1020% that inactivated *E. coli* completely within 90 min in the dark (Table 1 and Figure 4b). It follows that the Cu-loading percentage required in the Cu-nanoparticulate films sputtered by HIPIMS to inactivate *E. coli* completely was about three times lower compared with DCMS-sputtered Cu-nanoparticulate films.

Taking 0.3 nm as the lattice distance of Cu atoms, $\sim 10^{15}$ atoms/cm^2 can be estimated for one atomic layer ~0.2 nm thick.[30] With 60 amps, a layer 28 nm was deposited (Figure 2) within 61 s, equivalent to 140 layers with a content of 1.4×10^{17} atoms Cu/cm^2. This is a deposition ratio of 2.3×10^{15} atoms/cm^2 s.

Some recent work[23,24] has suggested a different number of O vacancies and or Cu vacancies in the Cu-nanoparticles HIPMS-sputtered at different energies to account for the different kinetics reported in Figure 4a,b for *E. coli* inactivation.

Cu Ions and Ar Ions Composition Sputtered by HIPIMS and DCMS Derived from Mass Spectroscopy Analysis. Figure 5 presents the ion composition when sputtering from the same Cu target by DCMS and HIPIMS in Ar, derived from mass spectroscopy analysis. By inspection of Figure 5, it is readily seen that the composition of the ions in the DCMS chamber gas phase was: 87% Ar^+, 5% Ar^{2+}, and 8% Cu^+. Low amounts of Cu^+ ions were found for the DCMS-sputtered samples in Figure 5. The amount of Cu^+ ions increases with HIPIMS at 6 amps to reach 97% along 3% Ar^{2+}. Finally, at 60 amps, the composition of the gas phase is: 17% Ar^+, 3% Ar^{2+}, 75% Cu^+, and 5% Cu^{2+}. The HIPIMS runs show that with increasing current the Ar^{2+} and the amount of Cu^{2+} in the gas phase increased.

During the magnetron sputtering, the ionization $Ar \rightarrow Ar^+ + e^-$ leads in a subsequent step to the collision of the electron with Cu: $e^- + Cu^0 \rightarrow Cu^+ + 2e^-$. The high-speed electron during the physical collision with the Cu kicks off a second electron, leading to the Cu^+ ion. In the case of HIPIMS, the electron/ions in the chamber are more likely due to the higher e-density to reach the entire polyester fiber compared with the DCMS[25] and DCMSP,[26] as reported recently. At 60 amps, the 2e collected at the polyester release a higher energy than the energy released at 6 amps during the settling of the Cu^+ ions on the polyester. To compare the sputtering energies, we used 700 W in DCMS on a target 7.6 cm^2 in diameter with a current density of 16.7 mA/cm^2. The current densities with HIPIMS at 6 and 60 amps (peak current values) presented higher values of 103.4 and 1034 mA/cm^2, respectively.

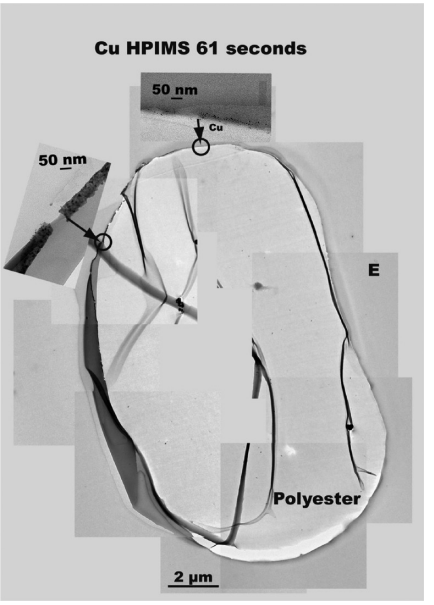

Figure 6. Electron microscopy of an Ag-polyester fiber HIPIMS-sputtered for 61 s at 60 amps. E stands for the epoxide used in the preparation of the sample.

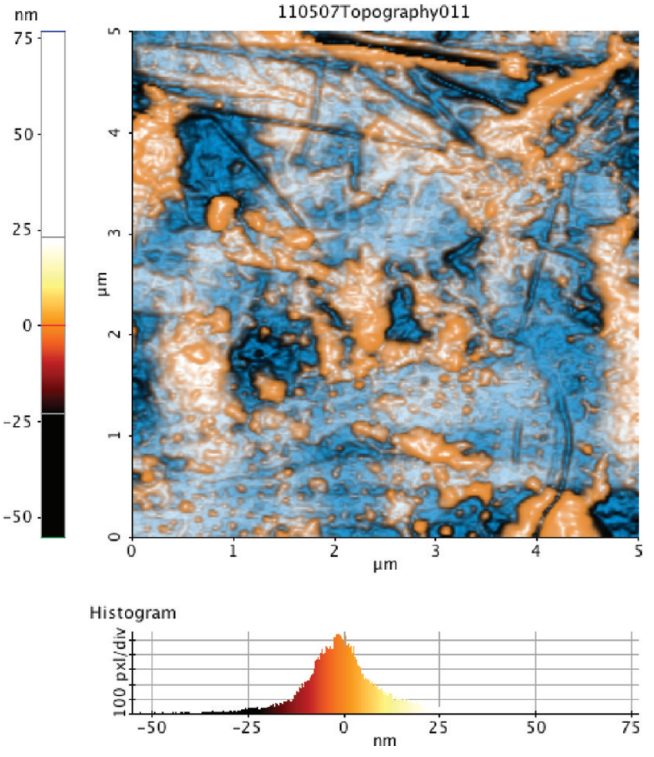

Figure 7. AFM of polyester/Cu taken in a field 5×5 μm R_q = 16.9 nm and R_a = 9.1 nm over 10 measurements. Darker regions show the valleys, and clear regions show the peaks of the surface film topography.

Electron Microscopy of the Cu-Nanoparticulate Films Sputtered by HIPIMS. Figure 6 shows the composite electron

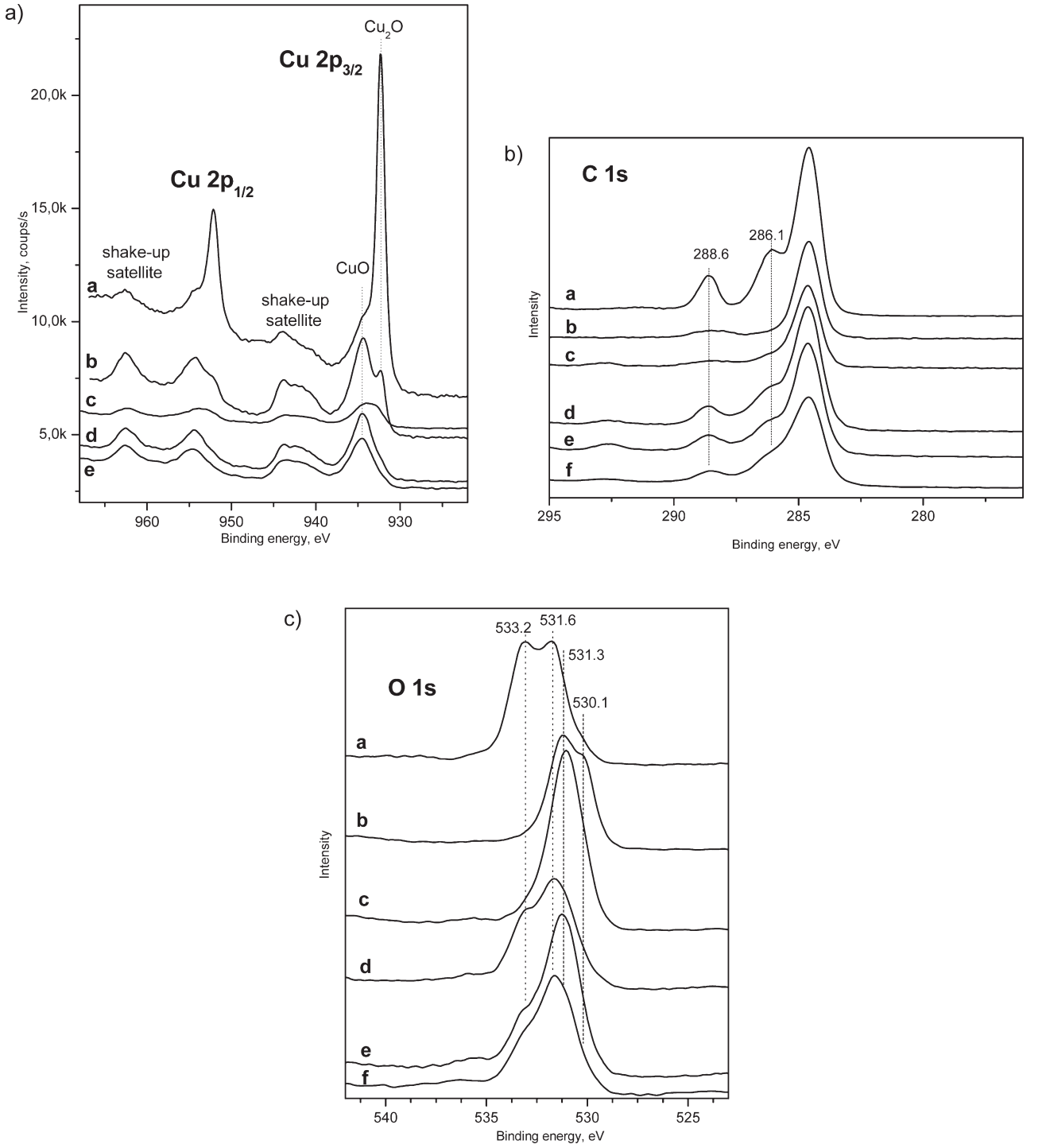

Figure 8. (a) XPS Cu2p doublet +2 shakeup satellites that represent two types of Cu: CuO at 934.1 eV and Cu_2O at 932.3 eV after for different samples: (a) polyester/Cu 0 min, (b) polyester/Cu + bacteria, 0 min, (c) polyester/Cu + bacteria, 30 min, (d) polyester/Cu + bacteria, 60 min, and (e) polyester/Cu + bacteria, 90 min. (b) XPS C1s (a) polyester, (b) polyester/Cu, (c) polyester/Cu + bacteria 0 min, (d) polyester/Cu + bacteria, 30 min, (e) polyester/Cu + bacteria, 60 min, and (f) polyester/Cu + bacteria, 90 min. (c) XPS O1s lines that represent two types of O in polyester/Cu, C═O at 531.6 eV and C−O at 533.2 eV, and two types of O in oxidized Cu, Cu−O at 530.1 eV and Cu_2O at 531.3 eV. The O from the bacteria at 531.0 eV should be considered. (a) polyester, (b) polyester/Cu, (c) polyester/Cu + bacteria, 0 min, (d) polyester/Cu + bacteria, 30 min, (e) polyester/Cu + bacteria, 60 min, and (f) polyester/Cu + bacteria, 90 min.

microscopy of Cu-nanoparticulate films sputtered for 61 s at 60 amps. The fiber is presented on a 2 μm scale, and the borders with the Cu nanoparticles were analyzed with a higher resolution (50 nm scale) along the perimeter of the fiber. The Cu layers varied between 10 and 35 nm when the fiber was exposed to the plasma flux coming directly from the target. Cu particle sizes between 5 and 10 nm are observed in Figure 1. The arrow in the left-hand side of Figure 1 shows the TEM of the thick Cu-particulate layer.

The thinnest Cu layers between 5 and 10 nm built up when the plasma flux reached the opposite side of the fiber. We followed the distribution of Cu layers taken 10 EM plates in different zones of the polyester fiber perimeter, and this allowed us to observe this section of Cu particles on the polyester fiber. This TEM section is presented under the top arrow in Figure 1, including Cu particle size very similar to the ones observed on the thick Cu layers described above

AFM of Polyester/Cu and Polyester/Cu-Bacteria after Initial Contact and 90 min. Figure 7 shows the AFM of polyester/Cu. The values of the R_q = 16.9 nm, and the root-mean-square of the rugosity was observed to be in experimental error similar to the R_q values found for Cu-nanoparticulate films contacted with *E. coli* for a few seconds or for 90 min. The arithmetic value of the rugosity R_a was 9.1 nm and was very similar to the R_a found for the polyester/Cu contacted with *E. coli* during short or long bacterial inactivation times. The values found for the rugosity indicate that the texture of the Cu film on the polyester is smooth. The histogram in Figure 7 shows the height of the Cu layer up to 500 pixels. The *x* axis shows the distribution of the peaks heights along in the *y* axis. Because the R_q values and the R_a were similar before and after the inactivation of *E. coli*, the stability of the Cu film seems not to be affected during bacterial inactivation. Therefore, no variation in the roughness and in the Cu-nanoparticulate film pore diameter would take place that may affect the bacterial attachment to the polyester/Cu surface.

XPS of the Polyester/Cu Samples As a Function of *E. coli* Inactivation Time. The sample in Figure 8a refers to polyester/Cu sputtered for 61s at 60 amps. Table 2 shows the surface atomic composition % for the main elements as a function of the bacterial inactivation time. The C in the Cu-nanoparticulate films at time zero decreases with respect to pure polyester because of the Cu coverage. When contacted with bacteria (third column), the C is seen to decrease again because of the Cu-degrading C-bacteria. At longer reaction times, the surface % of C stabilizes because of the presence of death bacteria and C residues up to 90 min. The Cu % present is seen to decrease after time zero because of the surface carbon stabilizing its presence up 90 min.

Figure 8a presents the spectrum of the Cu2p doublet with the shakeup satellites CuO at 934.1 and 932.3 eV.[28] As seen in Figure 8a and Table 3, at time zero, the majority of Cu exists as Cu_2O (71.2%), and CuO content is only 28.8%. Exposition to the bacterial suspension results in a strong oxidation of the Cu_2O to CuO (83.7%), but during the bacterial oxidation, the CuO on the polyester reduced after 30 min to 70% because of redox processes occurring in the dark on the Cu-nanoparticulate films when Cu comes in contact with *E. coli*. After a longer bacterial inactivation time, the CuO oxidizes again, increasing its presence to 94% when the bacterial inactivation is seen to be complete within 90 min (Figure 4b). At this point, the Cu-nanoparticulate film is ready to oxidize *E. coli* again. The results presented in Figure 8a and Table 3 describe the variation of the Cu^+ and Cu^{2+} as the bacterial inactivation progresses, suggesting a complex reaction mechanism taking place during the *E. coli* inactivation period.

Figure 8b presents the XPS C1s spectra for the polyester and Cu-nanoparticulate films contacted with *E. coli* during the bacterial inactivation period up to 90 min. XPS C1s line shows three components: C−C aromatic at 284.6 eV, C−O at 286.1 eV, and O−C═O at 288.6 eV characteristic for the polyester-Dacron (poly(ethylene terephthalate) (PET)) being used throughout this work. There is a significant modification of the line at 288.6 eV after Cu deposition (spectrum b). A very broad peak with an additional component at ∼287.5 eV suggests changes in the electrons distribution of the O−C═O group due to Cu deposition. This involves the partial reduction of carboxylic group O−C═O to carbonyl group C═O and has been reported by our laboratory.[34] The broadening of the O−C═O signal during *E. coli* inactivation suggests direct interaction of Cu with carboxylic groups. During the course of *E. coli* inactivation, the C1s line shows a different ratio between the carbon component at 286.1 and 288.6 eV.

Figure 8c shows the one-to-one doublet expected in the O1s line. Figure 8c shows the modification of the doublet during the *E. coli* inactivation starting with polyester alone, loading with Cu, and later contacting with the bacterial suspension up to bacterial inactivation. The $-OH_{surf}$ could not be specifically identified at 533 eV[28] because of the strong signal of the polyester shown in trace a in Figure 8c beside the signals due to the CuO and adsorbed bacteria. The increase in C−O (286.1 eV) and the decrease in C−C (284.6 eV) for polyester/Cu shown in Table 3 confirms (a) the growth of oxygen groups as the bacterial inactivation become longer and (b) some decrease in the C−C species on the polyester due to bacterial inactivation.

Table 2. Surface Atomic Composition Concentration % of the Main Elements on the Polyester Cu-Sputtered by HIPIMS for 61 s at 60 amps

sample	C	O	N	Cu	Na	P	Cl
polyester blank	75.30	23.13			1.21	0.36	
polyester + Cu, time zero	53.76	26.50		19.74			
polyester + Cu + bacteria, time zero	44.81	32.63	0.48	14.08	2.80	2.19	0.31
polyester + Cu + bacteria (30 min)	68.89	22.04	1.14	1.76	3.70	0.35	
polyester + Cu + bacteria (60 min)	60.29	25.90	0.35	4.59	3.15	0.93	
polyester + Cu + bacteria (90 min)	61.13	23.84	0.20	4.35	3.56	6.11	

Table 3. C and Cu Species on Polyester Cu Sputtered by HIPIMS for 61 s at 60 amps

sample	C−C 284.6 eV	C−O 286.1 eV	O−C═O 288.6 eV	Cu_2O 932.3 eV	CuO 934.1 eV
polyester blank	62.63	26.67	10.71		
polyester + Cu, time zero	80.74	10.47	9.07	71.19	28.81
polyester + Cu + bacteria, time zero	71.42	20.49	8.08	16.35	83.65
polyester + Cu + bacteria (30 min)	62.78	27.18	8.28	29.97	70.03
polyester + Cu + bacteria (60 min)	64.03	22.55	10.20	7.19	92.81
polyester + Cu + bacteria (90 min)	60.07	31.39	7.38	6.08	93.92

We suggest based on the evidence of the XPS data that the ROS of *E. coli* leading to bacterial inactivation is due to the redox interaction with Cu^{2+}/Cu^{1+} by reactions 1 and 2 below

$$Cu^{+} + O_2^{\cdot -} \Pi Cu^{0} + O_2 \quad (1)$$

$$Cu^{o} + O_2 \Pi Cu^{+} + O_2^{\cdot -} \quad (2)$$

The Cu^{2+} as Fe^{3+} is able to enhance the ROS formation via Fenton-like reaction[35]

$$Cu^{2+} + e_{cb}^{-} \Pi Cu^{+} \quad (3)$$

or by a two-electron transfer from Cu^{2+} leading to Cu^{o} atoms

$$Cu^{2+} + 2e^{-} \Pi Cu^{o} \quad (4)$$

The Cu atoms then coalesce to Cu^{0} nanoparticles settling in the Cu network of the cotton with $E_{redox} = -0.34$ V versus NHE.[36]

CONCLUSIONS

This study presents the first application of HIPIMS to prepare films with a controlled structure for bacterial inactivation showing the effect of the sputtering energy on the *E. coli* inactivation kinetics.

- The inactivation kinetics has been related to the Cu layer thickness and the layer rugosity.
- The redox catalysis involving Cu^{+}/Cu^{2+} and *E. coli* at the Cu-particulate film surface as a function of the reaction time is described quantitatively by XPS.
- The sputtered Cu layers have been characterized for Cu-particle size, layer thickness, amount of Cu deposited, light absorption (color), rugosity, and the organic transients during the bacterial inactivation process.
- A substantial saving of Cu when deposited by HIPIMS was required compared with Cu-deposited by DCMS to inactivate *E. coli* within similar times.
- A simple mechanism for the bacterial inactivation has been suggested, but the full mechanism is still uncertain. The information provided in this study will enable the readership to investigate further in the area of Cu biomaterials.

ACKNOWLEDGMENT

We wish to thank the COST Action MP0804 Highly Ionized Pulse Plasma Processes (HIPIMS) and the EPFL for the support of this work.

REFERENCES

(1) Foster, H. A.; Sheel, W. D.; Sheel, P.; Evans, P; Varghese, S.; Rutschke, N.; Yates, M. H. *J. Photochem. Photobiol., A* **2010**, *216*, 283–289.
(2) Dunlop, M. S. P.; Sheeran, P. C.; Byrne, A. J.; McMahon, S. A. M; Boyle, A. M.; McGuigan, G. K. *J. Photochem. Photobiol., A* **2010**, *216*, 303–3010.
(3) Kramer, A.; Schwebke, I.; Kampf, G. *BMC Infect. Dis.* **1997**, *6*, 130–138.
(4) Sunada, K.; Watanabe, K.; Hashimoto, K. *Environ. Sci. Technol.* **2003**, *37*, 4785–4789.
(5) Page, K.; Wilson, M.; Parkin, P. I. J. *Mater. Chem.* **2009**, *19*, 3819–3831 and references therein.
(6) Dancer, S. J. *J. Hosp. Infect.* **2009**, *73*, 378–385.
(7) Anita, S.; Ramachandran, T.; Rajendran, R.; Koushik, V.-C.; Mahalakshmi, M. *Textile Res. J.* **1011**, *81*, 1081–1088.
(8) Scholz, J.; Nocke, G.; Hollstein, F.; Weissbach, A. *Surf. Coat. Technol.* **2005**, *192*, 252–256.
(9) Shahidi, S.; Ghoranneviss, M.; Moazzenchi, B.; Rashidi, A. *Plasma Processes Polym.* **2007**, *4*, S1098–S1103.
(10) Wei, Q.; Li., Q.; Hou, D.; Yang, Z.; Gao, W. *Surf. Coat Technol.* **2006**, *201*, 1821–1826.
(11) Kiwi, J.; Pulgarin, C. In *Science and Technology against Microbial Pathogens. Research, Development, and Evaluation*; Mendez-Vilas, A., Ed.; World Scientific Publishing: 2011; pp 160−163.
(12) Kiwi, J.; Pulgarin, C. In *Science and Technology against Microbial Pathogens. Research, Development, and Evaluation*; Mendez-Vilas, A., Ed.; World Scientific Publishing: 2011; pp 186−1189.
(13) Park, J.; Jung, Y.; Cho, J.; Choi, W. *Appl. Surf. Sci.* **2006**, *252*, 5877–5891.
(14) Gao, F.; Pang, H.; Xu Sh., Lu, Q. *Chem. Commun.* **2009**, 3571–3573.
(15) Gabbay, J.; Borkow, G.; Mishal, J.; Magen, E.; Zatcoff, R.; Shemer-Avni, Y *Ind. Text.* **2006**, *35*, 223–227.
(16) Borkow, G.; Gabbay, J. *Med. Hypotheses* **2008**, *70*, 990–994.
(17) Borkow, G.; Gabbay, J. *FASEB J.* **2004**, *18*, 1728–1730.
(18) Gedanken, A *Ultrason. Sonochem.* **2004**, *11*, 47–53.
(19) Ehiasarian, P. A.; Vetushka, A.; Hecimovic, A; Konstantinidis, S. *J. Appl. Phys.* **2008**, *104*, 083305.
(20) Ehiasarian, P. A.; Gonzalvo, A. Y.; Whitmore, D. T. *Plasma Process. Polym.* **2007**, *4*, 5309–5313.
(21) Ehiasarian, P. A.; New, R.; Münz, D.-W.; Hultman, L.; Helmersson, U.; Kouznetsov, V. *Vacuum* **2002**, *65*, 147–154.
(22) Hopwood, J. *Thin Films Ionized Physical Vapor Deposition*; Academic Press: New York; Vol. 27; pp 181−205.
(23) Lin, J.; Moore, J.; Sproul, W.; Mishra, B.; Wu, Z.; Wang *Surf. Coat. Technol.* **2010**, *204*, 2230–2239.
(24) Sarakinos, K.; Alami, J.; Konstantinidis, S. *Surf. Coat. Technol.* **2010**, *204*, 1661–1684.
(25) Castro, C.; Sanjines, R.; Pulgarin, C.; Osorio, P.; Giraldo, A. S.; Kiwi, J. *J. Photochem. Photobiol., A.* **2010**, *216*, 295–302.
(26) Osorio, P.; Sanjines, R.; Ruales, R.; Castro, C.; Pulgarin, C.; Rengifo, J-A; Lavanchy, C.-J.; Kiwi, J. *J. Photochem. Photobiol., A.* **2011**, *220*, 70–76.
(27) Briggs, D.; Shea, M. *Practical Surface Analysis: Auger and X-ray Photoelectron Spectroscopy*, 2nd ed.; John Wiley & Sons: New York, 1988.
(28) *Handbook of X-Ray Photoelectron Spectroscopy*; Wagner, D. C., Riggs, W. M., Davis, L. E., Mullenberg, E. G., Eds.; Perkin-Elmer Corp. Physical Electronics Division: Eden Prairie, MN, 1979.
(29) Shirley, D. A. *Phys. Rev. B* **1972**, 4709–4716.
(30) Ch 4: Nucleation of Thin Films. In *Epitaxial Growth, Part B*; Mathews, J. W., Ed.; Academic Press, New York, 1975; pp 382−486.
(31) Kelly, P. J; Arnell, D. R. *Vacuum* **2000**, *56*, 159–172 and references therein.
(32) Hardee, K; Bard, A. *J. Electrochem. Soc.* **1977**, *124*, 215–224.
(33) Perelshtein, I.; Applerot, G.; Perkas, N.; Wehrschuetz-Sigl, E.; Hasmann, A.; Guebitz, G.; Gedanken, A. *Surf. Coat. Technol.* **2009**, *204*, 54–57.
(34) Dhananjeyan, M.; Mielczarski, E.; Thampi, K.; Buffat, Ph.; Bensimon, M.; Kulik, A.; Mielczarski, J.; Kiwi, J. *J. Phys. Chem. B* **2001**, *105*, 12046–12055.
(35) Fernandez, J.; Maruthamuthu, P.; Kiwi, J. *J. Photochem. Photobiol., A* **2004**, *161*, 185–191.
(36) Pourbaix, M. *Atlas of Electrochemical Equilibria in Aqueous Solutions*; Nace International Cebelcor: Brussels, 1974.